THE JOURNAL OF PHYSICAL CHEMISTRY A LETTERS

2009, *113,* 6540–6543
Published on Web 05/21/2009

Hydrogen Storage in Double Clathrates with *tert*-Butylamine

Pinnelli S. R. Prasad,[†,‡] Takeshi Sugahara,[†,§] Amadeu K. Sum,[†] E. Dendy Sloan,[†] and Carolyn A. Koh*[,†]

Center for Hydrate Research, Chemical Engineering Department, Colorado School of Mines, Golden, Colorado 80401, Gas Hydrates Division, National Geophysical Research Institute, Council for Scientific and Industrial Research, Hyderabad 500606, India, Division of Chemical Engineering, Graduate School of Engineering Science, Osaka University, Toyonaka, Osaka 560-8531, Japan

Received: April 1, 2009; Revised Manuscript Received: May 6, 2009

The first proof-of-concept of the formation of a double *tert*-butylamine (*t*-$BuNH_2$) + hydrogen (H_2) clathrate hydrate has been demonstrated. Binary clathrate hydrates with different molar concentrations of the large guest *t*-$BuNH_2$ (0.98−9.31 mol %) were synthesized at 13.8 MPa and 250 K, and characterized by powder X-ray diffraction and Raman microscopy. A structural transformation from sVI to sII of *t*-$BuNH_2$ hydrate was clearly observed under hydrogen pressures. Raman spectroscopic data suggested that the hydrogen molecules occupied the small cages and had similar occupancy to hydrogen in the double tetrahydrofuran (THF) + H_2 clathrate hydrate. The hydrogen storage capacity in this system was ∼0.7 H_2 wt % at the molar concentration of *t*-$BuNH_2$ close to the sII stoichiometry.

Introduction

Significant challenges still remain in the development of suitable materials for storing molecular hydrogen (H_2) for practical applications. Clathrate hydrates are a class of inclusion compounds among other materials, such as metal hydrides, metal-organic framework, carbon based, and noncarbon nanomaterials, which have been considered for their potential to store hydrogen.[1,2] Clathrate hydrate materials could be tailored to reduce the storage pressure and temperature to near ambient conditions, though the storage capacity is typically also decreased. In addition to the most common structure I (sI), structure II (sII), and structure H (sH) gas hydrates,[3] several other clathrate structures denoted sI to structure VII (sVII) were proposed by Jeffery.[4] These structures, with the exception of structures IV and V, have been experimentally verified. Examples of guest molecules forming these different structures are methane for sI, propane or tetrahydrofuran (THF) for sII, Br_2 for structure III, *tert*-butylamine (*t*-$BuNH_2$) for structure VI (sVI), hexafluorophoric acid for sVII, and methylcyclohexane for sH.

In the study by Strobel et al.,[5] the hydrogen storage capacity for the different clathrate structures has been estimated by assuming multiple occupancy in the cages (depending on cage size). From those calculations, sVI hydrate is the only clathrate structure with an estimated storage capacity approaching the U.S. DOE target of 6 wt %, assuming full occupancy of the small cages and fractional occupancy (>0.8) of the large cages with hydrogen in sVI. Table 1 summarizes the ideal H_2 storage capacity for the different known clathrate hydrate structures.

TABLE 1: Ideal H_2 Storage Capacity in the Different Known Hydrate Structures

		averaged H_2 occupancy per		
hydrate system	structure	small cage(s)	large cage	H_2 capacity/ wt %
t-$BuNH_2$ + H_2	sVI	1	4.5 (=0.75 × 6)[a]	5.18
t-$BuNH_2$ + H_2	sVI	1	3 (=0.50 × 6)[a]	3.45
t-$BuNH_2$ + H_2	sVI	1	0	0.61
t-$BuNH_2$ + H_2	sII	1	0	1.05
pure H_2	sII	2	4	5.01
pure H_2	sII	1	4	3.81
MTBE[b] + H_2	sH	1	0	1.42
1,1-DMCH[c] + H_2	sH	1	0	1.37
THF[d] + H_2	sII	1	0	1.06

[a] The assumption is that a cluster of six H_2 molecules partially occupies the large cages of sVI by the tuning effect. The numbers of 0.75 and 0.50 are the hypothetical large cage occupancy. [b] MTBE = methyl-*tert*-butyl ether. [c] DMCH = dimethylcyclohexane. [d] THF = tetrahydrofuran.

Recently, Kim et al.[6] have reported a structural transformation in sVI *t*-$BuNH_2$ hydrates [16 *t*-$BuNH_2 \cdot 156\ H_2O$] to sII upon pressurization with methane at 70 bar and 283.65 K, thus raising the question of whether hydrogen, a smaller molecule, would induce a similar structural transformation. If the sVI can be preserved upon pressurization with a small guest molecule that would occupy both small and large cages, sVI clathrate would be a favorable material for hydrogen storage. However, controversy still remains on the occupancy of the small and large cages,[7] with some reports claiming two H_2 molecules per small cage (5^{12}),[8] while experimental results from other groups have been interpreted by considering a single H_2 molecule in the small cages.[9−13]

The maximum H_2 storage capacity of pure hydrogen hydrates with single occupancy of the small cages and multiple occupancy of the large cages is 3.8 wt %. Pure hydrogen hydrates

* Corresponding author. Fax: +1 (303) 273-3730. Phone: +1 (303) 273-3237. E-mail: ckoh@mines.edu.
[†] Colorado School of Mines.
[‡] National Geophysical Research Institute.
[§] Osaka University.

10.1021/jp9029997 CCC: $40.75

typically require very high pressure (~200 MPa) and low temperature conditions.[18] Conversely, the formation pressure can be considerably reduced in binary clathrates in which large cages are occupied by a large guest, such as THF.[10] In such cases, the maximum achievable hydrogen storage capacity is around 1 wt % when all of the small cages are singly occupied by hydrogen.[13,16,17] Current research in this area focuses on finding new materials, among true clathrates, semiclathrates, and hybrid clathrates, which demonstrate higher hydrogen storage capacity and increased stability under near ambient pressure and temperature conditions.

The main aim of the present study was to show the first proof-of-concept of hydrogen enclathration in *t*-$BuNH_2$ hydrate, a sVI clathrate, and investigate possible structural transformation from sVI induced by the presence of a small guest molecule. While *t*-$BuNH_2$ hydrate was studied previously with methane as a small cage guest,[6,19] there are no reports on hydrogen enclathration with this particular system. The results in this study report an unexpected structural transition of sVI *t*-$BuNH_2$ hydrates to sII even when the system was pressurized with guests small enough in molecular size to occupy the small cages of sVI. Evidence for these findings was obtained from Raman spectral signatures of the enclathrated guest molecules, powder X-ray diffraction, and volumetric storage measurements.

Experimental Method

The *t*-$BuNH_2$ clathrate hydrate samples were synthesized from specific amounts (0.98−9.31 mol %) of *t*-$BuNH_2$ (Sigma-Aldrich) and deionized water at 258 K and ambient pressure. The solution was vigorously stirred until hydrates formed, at which point, the hydrates were stored in a freezer at ~250 K for about 10−15 h. The hydrate (finely ground powder) was added to a pressure vessel which was precooled to below 200 K. The cell was pressurized with hydrogen gas (13.8 MPa) while maintaining the temperature at 250 K, for formation of the double (*t*-$BuNH_2$ + H_2) hydrate in the solid state. The cell was maintained at these conditions over a period of 48 h (temperature constant at 250 K) for the enclathration of H_2 into the hydrate. The cell was immersed in liquid nitrogen for about 15−20 min, degassed, and then the double hydrate was analyzed by powder X-ray diffraction (PXRD) and Raman spectroscopy.

The PXRD was measured on a Siemens D500 diffractometer with Co radiation (wavelength 1.788965 Å) in the $\theta/2\theta$ scan mode. The measurements were done in the step scan mode with a dwell time of 2 s and step size of 0.02°. The PXRD pattern was collected in the range $2\theta = 8-65°$; measurements were carried out at ambient pressure and 100 K. The Raman spectroscopic measurements were performed using a LabRam HR spectrometer (JY Instruments) with a 532 nm excitation source providing 6 mW at the sample. All of the measurements were recorded at ambient pressure and near liquid nitrogen temperature.

For the volumetric gas release measurements, the double hydrates were prepared using a similar procedure to that described above, i.e., by using finely ground (~200 μm) *t*-$BuNH_2$ hydrates pressurized with H_2 at about 50 MPa. Residual gas in the cell was decreased to atmospheric pressure at around ~200 K. The cell was connected to a gasometer (Ruska Inc.) to measure the amount of gas released. The maximum uncertainty of the measured amount of gas was about 10% for samples with nearly the same *t*-$BuNH_2$ molar concentration.

TABLE 2: Ratio of Molecular Diameter to Cage Diameter for the Guest Molecules of sII and sVI Clathrates[a]

	structure II		structure VI	
	5^{12} (7.82 Å)	$5^{12}6^4$ (9.46 Å)	4^45^4 (5.80 Å)	$4^35^96^27^3$ (10.2 Å)
H_2 (2.72 Å)	0.542	0.408	0.907	0.368
CH_4 (4.36 Å)	0.868	0.655	1.453	0.589
t-$BuNH_2$ (6.72 Å)	1.339	1.009	2.240	0.908

[a] Diameters of the cages and guest molecules are shown in parentheses. Data compiled from refs 3 and 5. The ratio is calculated by subtracting the diameter (2.80 Å) of water molecules from the cage diameter.

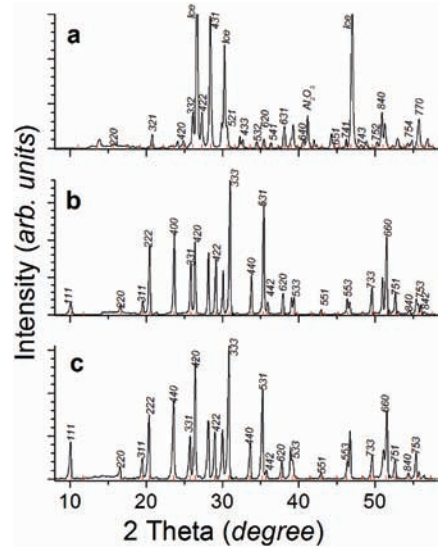

Figure 1. Powder X-ray diffraction patterns of pure *t*-$BuNH_2$ (a) and double (*t*-$BuNH_2$ + H_2) hydrates with *t*-$BuNH_2$ 5.86 mol % (b) and 8.86 mol % (c) recorded at ambient pressure and 100 K. The pure *t*-$BuNH_2$ clathrate hydrate was pressurized with hydrogen (13.8 MPa and 250 K). Vertical bars at the bottom of each graph represent the generated 2θ values using the optimized unit cell parameters (see text).

Results and Discussion

The *t*-$BuNH_2$ clathrate hydrate is known to crystallize into a cubic sVI hydrate, which consists of two types of cages: 8-hedra (4^45^4) and 17-hedra ($4^35^96^27^3$). The diameter for small and large cages is 5.8 and 10.2 Å, respectively (see Table 2). In sVI hydrate, *t*-$BuNH_2$ molecules occupy the large cages, leaving the small cages vacant. As shown in Table 2, an analysis of the size constraints for small guests in the sVI cages shows that it is impossible to fill the small cages (4^45^4) of sVI with methane (size ratio is 1.453). However, the corresponding size ratio for hydrogen in the small cage of sVI is 0.907, thus suggesting that the structure could be more stable, from size arguments, when the empty cages are filled with a coguest such as hydrogen. As discussed earlier, a structural transformation from sVI to sII in double (*t*-$BuNH_2$ + CH_4) hydrate was previously reported.[6] Here, we investigated the *t*-$BuNH_2$ hydrate with H_2 as a coguest molecule to possibly occupy the small cages of sVI.

The PXRD patterns of pure *t*-$BuNH_2$ and *t*-$BuNH_2$ + H_2 hydrates are shown in Figure 1. The PXRD pattern indexing and cell refinement were obtained using the Checkcell & PowderX programs.[20] As seen in Figure 1a, it is clear that the starting material, synthesized with 5.86 mol % *t*-$BuNH_2$, can be indexed to sVI, indicating that the *t*-$BuNH_2$ hydrates crystallized into a cubic $I\bar{4}3d$ structure even when the mole

fraction is less than the stoichiometric composition of 9.31 mol %. An earlier reported parameter ($a = 18.81$ Å[4,6]) was used as an initial guess value to obtain the refined unit cell parameter of $a = 18.5711 \pm 0.0202$ Å. The vertical bars in Figure 1 indicate the generated 2θ values. A similar procedure was used to analyze the PXRD data for the double *t*-$BuNH_2 + H_2$ clathrate hydrates. The resulting PXRD pattern for *t*-$BuNH_2$ (5.86 mol %) + H_2 hydrates (Figure 1b) was better fitted to a sII hydrate (space group *Fd3m*) with a lattice constant of $a = 17.4443 \pm 0.0135$ Å. We also observed a similar PXRD pattern for *t*-$BuNH_2$ (8.86 mol %) + H_2 hydrates (Figure 1c), which was also indexed to sII with $a = 17.4898 \pm 0.0225$ Å. Negligible amounts of unconverted sVI were identified in the patterns for the double *t*-$BuNH_2 + H_2$ hydrates. From the PXRD results, it is evident that a structural transformation from sVI to sII occurred when hydrate samples initially with only *t*-$BuNH_2$ were pressurized with H_2, even though H_2 is theoretically capable of populating the small cages (4^45^4) in sVI (see Table 2). The pure sVI *t*-$BuNH_2$ hydrate melts at 272 K.[4] It is known that certain double hydrates with completely occupied cages are stable up to higher temperatures compared to hydrates with partially vacant cages.[21,22] From Table 2, it is clear that hydrogen is small enough to fill the small cages of sVI, whereas methane, being a larger molecule, can possibly trigger the structural transformation. Kim et al.[6] have reported the coexistence of sVI and sII for *t*-$BuNH_2$ concentrations between 7.0 and 9.31 mol % in the double (*t*-$BuNH_2 + CH_4$) hydrate system, whereas sII was the preferred structure at lower concentrations (5.6−4.5 mol %) of the large guest molecule.

By considering the size of the guest molecules and the available cage sizes, it is suggested that the *t*-$BuNH_2$ molecules can occupy the large cages of both sVI (size ratio of 0.908) and sII (size ratio of 1.009); see Table 2. On the other hand, the hydrogen molecule could be conveniently stored in the small cages of sVI (size ratio of 0.907), and as is evident from the above criteria that only one molecule could occupy the 4^45^4 cage. Earlier studies on the double (5.6 mol % *t*-$BuNH_2 + CH_4$) hydrate by Kim et al.[6] showed that *t*-$BuNH_2$ can also occupy the $5^{12}6^4$ cages of sII. As described, the PXRD pattern on double hydrates *t*-$BuNH_2 + H_2$ also showed a structural transformation from sVI to sII. To better understand the enclathration of hydrogen in the hydrate structure, Raman microscopy was used to investigate the occupancy of the enclathrated hydrogen molecules. Figures 2 and 3 show the Raman spectra in the rotational and vibrational mode regions, respectively, for the enclathrated hydrogen molecules.

Figure 2 shows the Raman spectra of the H_2 rotational mode region of the double *t*-$BuNH_2 + H_2$ hydrates at two different concentrations of *t*-$BuNH_2$. These are compared with the spectral features for the double THF + H_2 hydrate and also with pure H_2 gas (vertical bars). The H_2 rotational modes for the double hydrates are downshifted (red shift) compared to the gas phase [$S_0(0)$ and $S_0(1)$ in the gas phase are at 354 and 587 cm^{-1}, respectively] and are significantly broader. The H_2 rotational modes for the *t*-$BuNH_2 + H_2$ hydrate are very similar to THF + H_2 hydrates,[9,10,14] and in the present study, the rotational modes are around 355 cm^{-1} [$S_0(0)$] and 582 cm^{-1} [$S_0(1)$]. The $S_0(0)$ band consists of at least three components. The results also indicate that the band positions are less dependent on the molar concentration of *t*-$BuNH_2$. Additionally, the total width of this mode is broader (~18 cm^{-1}) compared to THF + H_2 hydrates (~14 cm^{-1}). The results are also consistent with inelastic neutron scattering, Raman scattering, and molecular simulation studies which report that the $S_0(0)$ mode is degenerate

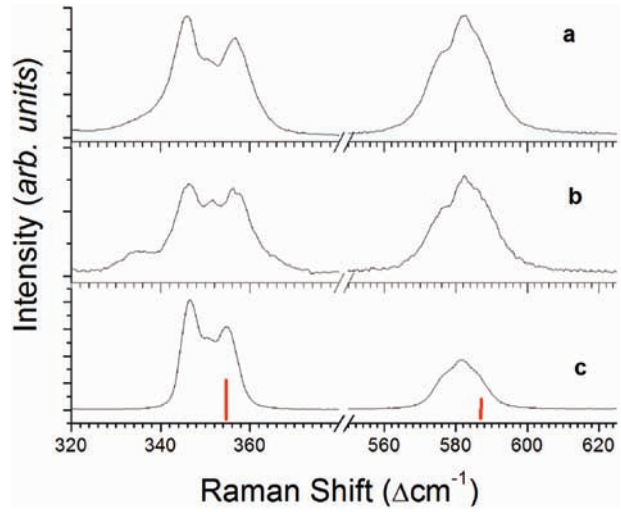

Figure 2. Raman spectra of double *t*-$BuNH_2 + H_2$ hydrates in the H_2 rotational mode region with *t*-$BuNH_2$ 0.98 mol % (a) and 8.86 mol % (b). The spectra were recorded at 100 K and atmospheric pressure. For comparison, the spectra of the THF + H_2 binary hydrate (c) and gas phase H_2 (vertical bars) are also shown.

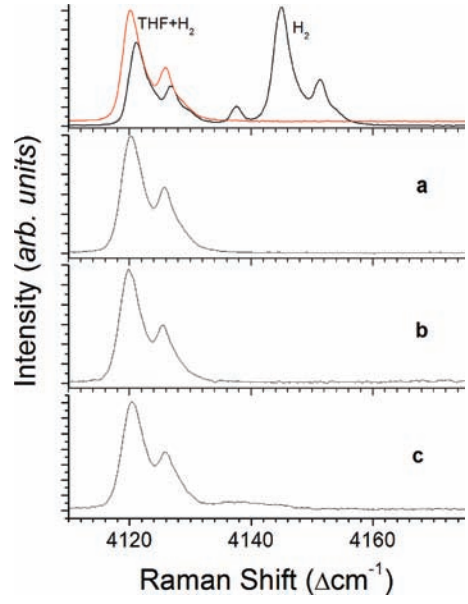

Figure 3. Raman spectra of enclathrated H_2 (vibron) molecules in double *t*-$BuNH_2 + H_2$ hydrates with *t*-$BuNH_2$ 0.98 mol % (a), 5.86 mol % (b), and 8.86 mol % (c). The spectra are recorded at 100 K and atmospheric pressure. For comparison, the vibron spectra of THF−H_2 and pure H_2 hydrates are also shown (top).

and splits into several (3−5) components at lower temperatures.[23,24] It is interesting to note that a similar width has been reported from earlier Raman (~16 cm^{-1}) and neutron scattering (~18 cm^{-1}) studies for THF + H_2 hydrates.[23]

The Raman spectrum for the H−H vibrons is also used as a fingerprint signature for H_2 molecules enclathrated in hydrate systems. At low temperatures near liquid nitrogen temperature, the Raman modes around 4120 cm^{-1} are generally assigned to H_2 molecules in small (5^{12}) cages, while the modes around 4130−4160 cm^{-1} are assigned to H_2 molecules in large ($5^{12}6^4$) cages.[5] As shown in Figure 3, the H−H vibrons for hydrogen molecules in the small cage can be clearly identified. Two of the *Q* branch vibrational modes, $Q_1(0)$ and $Q_1(1)$, of enclathrated H_2 are assigned to *ortho*- and *para*-hydrogen. The observed peak separation (~5.5 cm^{-1}) and the intensity ratio of these two

modes are consistent with earlier reports.[5,11,14] The vibron modes are unaffected by the *t*-$BuNH_2$ molar concentration. The Raman spectrum for double *t*-$BuNH_2$ 8.86 mol % + H_2 hydrates (close to sVI stoichiometry) is similar to that with 5.86 mol % (close to sII stoichiometry) and 0.98 mol %. It is typically observed that the vibrational modes of hydrogen in hydrates shift to lower wavenumbers as the cage size decreases, contrary to usual guest−cage behavior,[25] and thus, the H−H vibron modes for hydrogen molecules enclathrated in 4^45^4 or 5^{12} cages of sVI or sII, respectively, should show some shift in their peak positions. The observed spectral signatures for the double hydrates of H_2 with *t*-$BuNH_2$ and THF are very similar, indicating that the hydrogen molecules are enclathrated mostly in the 5^{12}-cage-like environment. This observation is further confirmation that the sVI hydrate undergoes a structural transformation to sII even when pressurizing with a coguest molecule suitable for occupying 4^45^4 cages.

To obtain an estimate of the hydrogen storage in the double *t*-$BuNH_2$ + H_2 hydrates, the amount of gas released from the hydrates (synthesized at 50 MPa) was measured with a different molar concentration of *t*-$BuNH_2$ in the range 1.67−9.31 mol %. The results show that the storage capacity of hydrogen in hydrates is very low (0.07 wt %) with the *t*-$BuNH_2$ concentration close to the sVI stoichiometry (8.86 mol %). Gas released from these samples was 10 ± 4 mL H_2/g *t*-$BuNH_2$ hydrate, at 0.82 atm pressure and 297 K. Such significantly low capacity cannot be only explained by the coexistence of excess *t*-$BuNH_2$. Note that, from PXRD results, almost all hydrate crystals are sII, not sVI. In the *t*-$BuNH_2$ concentration closer to sII stoichiometry (5.56 mol %), we measured 101 ± 4 mL H_2/g *t*-$BuNH_2$ hydrate, at 0.82 atm pressure and 297 K, for a total amount of hydrogen released (0.7 wt %) from the hydrate samples comparable with the double THF + H_2 hydrates measured around 50 MPa.[15,21,26,27]

Conclusions

The results shown here demonstrate that hydrogen can be enclathrated into the empty small cages of *t*-$BuNH_2$ hydrates. The structure transformation (sVI to sII) of *t*-$BuNH_2$ hydrate pressurized with hydrogen was clearly observed from the PXRD patterns. The Raman spectroscopic data suggested that the hydrogen molecules occupy the small cages of sII and have similar occupancy to hydrogen in double THF + H_2 hydrates. The hydrogen storage capacity was 0.7 wt % in the double *t*-$BuNH_2$ + H_2 hydrates at the molar concentration of the *t*-$BuNH_2$ near the sII stoichiometry.

Acknowledgment. The authors acknowledge the funding from NSF-REMRSEC [DMR 0820518]. P.S.R.P. is thankful to the Director, NGRI Hyderabad, for granting the sabbatical leave in the Center for Hydrate Research at the Colorado School of Mines. A.K.S. acknowledges the support from DuPont as a DuPont Young Professor.

References and Notes

(1) Schlapbach, L.; Zuttel, A. *Nature* **2001**, *414*, 353–358.
(2) van der Berg, A. W. C.; Arean, C. O. *Chem. Commun.* **2008**, 0668–681.
(3) Sloan, E. D.; Koh, C. A. Clathrate hydrates of natural gases, 3rd ed.; CRC Press, Taylor & Francis Gp.: Boca Raton, FL, 2008.
(4) McMullan, R. K.; Jeffrey, G. A.; Jordan, T. H. *J. Chem. Phys.* **1967**, *47*, 1229–1234.
(5) Strobel, T. A.; Koh, C. A.; Sloan, E. D. *Fluid Phase Equilib.* **2007**, *261*, 382–389.
(6) Kim, D. Y.; Lee, J.; Seo, Yu.-T.; Ripmeester, J. A.; Lee, H. *Angew. Chem.* **2005**, *117*, 7927–7930.
(7) Struzhkin, V. V.; Militzer, B.; Mao, W. L.; Mao, H.-k.; Hemley, R. J. *Chem. Rev.* **2007**, *107*, 4133–4151.
(8) Mao, W. L.; Mao, H.-k.; Goncharov, A. F.; Struzhkin, V. V.; Guo, Q.; Hu, J.; Shu, J.; Hemley, R. J.; Somayazulu, M.; Zhao, Y. *Science* **2002**, *297*, 2247–2249.
(9) Strobel, T. A.; Hester, K. C.; Sloan, E. D.; Koh, C. A. *J. Am. Chem. Soc.* **2007**, *129*, 9544–9545.
(10) Florusse, L. J.; Winans, Peters, C. J.; Schoonman, J.; Hester, K. C.; Koh, C. A.; Dec, S. F.; Marsh, K. N.; Sloan, E. D. *Science* **2004**, *360*, 469–471.
(11) Strobel, T. A.; Koh, C. A.; Sloan, E. D. *J. Phys. Chem. B* **2008**, *112*, 1885–1887.
(12) Lokshin, K. A.; Zhao, Y.; He, D.; Mao, W. L.; Mao, H.; Hemley, R. J.; Lobanov, M. V.; Greenblatt, M. *Phys. Rev. Lett.* **2004**, *93*, 125503–1.
(13) Senadheera, L.; Conradi, M. S. *J. Phys. Chem. B* **2008**, *112*, 13695–13700.
(14) Giannasi, A.; Celli, M.; Ulivi, L.; Zoppi, M. *J. Chem. Phys.* **2008**, *129*, 084705−1.
(15) Strobel, T. A.; Taylor, C. J.; Hester, K. C.; Dec, S. F.; Koh, C. A.; Miller, K. T.; Sloan, E. D. *J. Phys. Chem. B* **2006**, *110*, 17121–17125.
(16) Ogata, K.; Hashimoto, S.; Sugahara, T.; Moritoki, M.; Sato, H.; Ohgaki, K. *Chem. Eng. Sci.* **2008**, *63*, 5714–5718.
(17) Hasimoto, S.; Sugahara, T.; Sato, H.; Ohgaki, K. *Chem. Eng. Data* **2007**, *52*, 517–520.
(18) Dyadin, Yu.A.; Larinov, E. G.; Aladko, E. Y.; Manakov, A. Yu.; Zhurko, F. V.; Mikina, T. V.; Komarov, V. Y.; Grachev, E. V. *J. Struct. Chem.* **1990**, *40*, 790–795.
(19) Kim, D. Y.; Park, Y.; Lee, H. *Catal. Today* **2007**, *120*, 257–261.
(20) The software programmes Checkcell developed by Laugier, L.; Bochu, B. Laboratoire des Materiaux et du Genie Physique, Ecole Superieure de Physique de Grenoble and PowderX developed by Cheng, D. Institute of Physics, Beijing, are available at http://www.ccp14.ac.uk.
(21) Anderson, R.; Chapoy, A.; Tohidi, B. *Langmuir* **2007**, *23*, 3440–3444.
(22) Prasad, P. S. R.; Sowjanya, Y.; Prasad, K. S. Vib. Spectrosc. [Online early access]. DOI: 10.1016/j.vibspec.2009.02.003. Published Online: Mar 5, 2009.
(23) Ulivi, L.; Celli, M.; Giannasi, A.; Ramirez-Cuesta, A. J.; Zoppi, M. *J. Phys.: Conf. Ser.* **2008**, *121*, 042018 1−7.
(24) Xu, M.; Sebastianelli, F.; Bacic, Z. *J. Phys. Chem. A* **2007**, *111*, 12763–12771.
(25) Subramanian, S.; Sloan, E. D. *J. Phys. Chem. B* **2002**, *106*, 4348–4355.
(26) Nagai, Y.; Yoshioka, H.; Ota, M.; Sato, Y.; Inomata, H.; Smith, R. L., Jr.; Peters, C. J. *AIChE J.* **2008**, *54*, 3007–3016.
(27) Mulder, F. M.; Wagemaker, M.; van Eijck, L.; Kearley, G. J. *ChemPhysChem* **2008**, *9*, 1331–1337.

JP9029997